

DEMON: Improved Neural Network Training with Momentum Decay

John Chen
Rice University
USA
johnchen@rice.edu

Zhao Li
UTHealth
USA
Zhao.Li@uth.tmc.edu

Cameron Wolfe
Rice University
USA
wolfe.cameron@rice.edu

Anastasios Kyrellidis
Rice University
USA
anastasios@rice.edu

ABSTRACT

Momentum is a widely used technique for gradient-based optimizers in deep learning. In this paper, we propose a decaying momentum (DEMON) rule. We conduct the first large-scale empirical analysis of momentum decay methods for modern neural network optimization, in addition to the most popular learning rate decay schedules. Across 28 relevant combinations of models, epochs, datasets, and optimizers, DEMON achieves the highest number of Top-1 and Top-3 finishes at 39% and 85% respectively, almost doubling the second-placed learning rate cosine schedule at 17% and 60%, respectively. DEMON also outperforms other widely used schedulers including, but not limited to, the learning rate step schedule, linear schedule, OneCycle schedule, and exponential schedule. Compared with the widely used learning rate step schedule, DEMON is observed to be less sensitive to parameter tuning, which is critical to training neural networks in practice. Results are demonstrated across a variety of settings and architectures, including image classification, generative models, and language models. DEMON is easy to implement, requires no additional tuning, and incurs almost no extra computational overhead compared to the vanilla counterparts. Code is readily available.

KEYWORDS

Neural networks, deep learning optimization, image classification, language models

1 INTRODUCTION

Motivation. Deep Neural Networks (DNNs) have advanced the state-of-the-art in computer vision [23, 34, 51], natural language processing [6, 19, 42] and speech recognition [54, 56], but have come with huge computation costs. A state-of-the-art language model can cost several million USD to train [9, 59]. For most practitioners, even moderate tasks can be prohibitive in time and cost when the hyperparameter tuning process is taken into account, where it is typical to retrain models many times to achieve optimal performance.

In an effort to ease the cost of training DNNs, adaptive gradient-based methods [18, 25, 32, 41, 80] were devised. Cases exist where their use leads to degraded performance [57, 75], but this can be a result of poor hyperparameter tuning [2, 12, 57, 61]. Currently, SGD with momentum (SGDM) and Adam [32] remain among the

Table 1: Performance of different schedules ranked according to the % of Top-1 or Top-3 finishes, out of a total of 28 experiments. Top-1 refers to the best performance for a particular model-dataset-base optimizer-epoch setting. Top-3 refers to among the best 3 performances. E.g. RN20-CIFAR10-SGDM-300epochs would be considered one experiment. NCSN-CIFAR10, RN56-TINYIMAGENET and BERT_{BASE}-GLUE not included due to limited runs.

Method	Top-1 Performance	Top-3 Performance
OneCycle Momentum	0%	0%
Linear Momentum	0%	0%
Exp Momentum decay	0%	0%
Cosine Momentum	0%	3.57%
LR Exp decay	7.14%	10.71%
LR Decay on Plateau	7.14%	21.43%
OneCycle	7.14%	25.00%
LR Linear Schedule	10.71%	39.29%
LR Step Schedule	10.71%	53.57%
LR Cosine Schedule	17.86%	60.71%
DEMON	39.29%	85.71%

most popular methods for training DNNs. Many state-of-the-art benchmarks in Computer Vision are achieved using SGDM and a curated learning rate step schedule [23, 27, 29, 34, 51, 77, 79]. Meanwhile, variants of Adam are popular for training state-of-the-art language models [9, 16].

For optimizers to achieve good performance, their hyperparameters must be tuned properly. For example, slight changes in learning rate, learning rate decay, momentum, and weight decay (amongst others) can drastically alter performance. One key component to hyperparameter tuning is the selection of a good learning rate, and possibly momentum, decay schedule. Performance can vary substantially depending on this schedule, and, as we demonstrate, *no one schedule is optimal*. However, there is significant opportunity to improve upon existing schedules by fostering consistent state-of-the-art performance and robustness to hyperparameters across domains.

Momentum tuning. In this work, we focus on improving model performance and hyperparameter robustness with simple techniques for the momentum parameter. Momentum was designed to speed up learning in directions of low curvature, without becoming

Algorithm 1 DEMON in SGDM

Parameters: T number of iterations, step size η , initial mom. β_{init} . $v_0 = \theta_0 = 0$ or random.

for $t = 0, \dots, T$ **do**

$$\beta_t = \beta_{\text{init}} \cdot \frac{\left(1 - \frac{t}{T}\right)}{\left(1 - \beta_{\text{init}}\right) + \beta_{\text{init}} \left(1 - \frac{t}{T}\right)}$$

$$\theta_{t+1} = \theta_t - \eta g_t + \beta_t v_t$$

$$v_{t+1} = \beta_t v_t - \eta g_t$$

end for

Algorithm 2 DEMON in Adam

Parameters: T, η , initial mom. $\beta_{\text{init}}, \beta_2, \varepsilon = 10^{-8}$. $v_0 = \theta_0 = 0$ or random.

for $t = 0, \dots, T$ **do**

$$\beta_t = \beta_{\text{init}} \cdot \frac{\left(1 - \frac{t}{T}\right)}{\left(1 - \beta_{\text{init}}\right) + \beta_{\text{init}} \left(1 - \frac{t}{T}\right)}$$

$$\mathcal{E}_{t+1}^{g \circ g} = \beta_2 \cdot \mathcal{E}_t^{g \circ g} + (1 - \beta_2) \cdot (g_t \circ g_t)$$

$$m_{t,i} = g_{t,i} + \beta_t m_{t-1,i}$$

$$\theta_{t+1,i} = \theta_{t,i} - \frac{\eta}{\sqrt{\mathcal{E}_{t+1,i}^{g \circ g} + \varepsilon}} \cdot m_{t,i}$$

end for

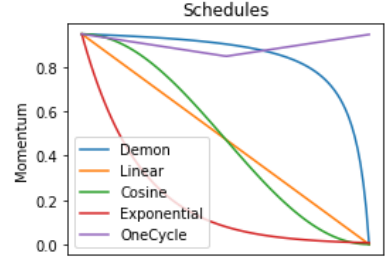


Figure 1: Non-linear DEMON schedule vs. other schedules, from $\beta_{\text{init}} = 0.9$ to 0.

unstable in directions of high curvature. To minimize the objective function $\mathcal{L}(\cdot)$, the most common momentum method, SGDM, is given by the following recursion:

$$\theta_{t+1} = \theta_t + \eta v_t, \quad v_t = \beta v_{t-1} - g_t.$$

for variable $\theta_t \in \mathbb{R}^p$, where β is the momentum, g_t is a stochastic gradient, where $\mathbb{E}[g_t] = \nabla \mathcal{L}(\theta_t)$, and $\eta > 0$ is the step size.

Practitioners set $\beta = 0.9$. This is supported by recent works [11, 25, 32, 50], and by the fact that most common softwares, such as PyTorch [47], use $\beta = 0.9$ as the default momentum value. *There is no indication that this choice is universally well-behaved.*

There are papers that attempt to tune the momentum parameter. In the distributed setting, [44] observe that running SGD asynchronously is similar to adding a momentum-like term to SGD. They provide empirical evidence that setting $\beta = 0.9$ results in a momentum “overdose”, yielding suboptimal performance. YellowFin [81] is a learning rate and momentum adaptive method for both synchronous and asynchronous settings, motivated by a quadratic model analysis and some robustness insights. Finally, in training generative adversarial networks (GANs), optimal momentum values tend to decrease from $\beta = 0.9$ [4, 43, 48], taking even negative values [22].

This paper. We perform the first large-scale empirical analysis of momentum decay methods and introduce the DEMON momentum decay rule, a novel method which performs favorably and increases hyperparameter robustness in comparison to other learning rate and momentum schedules. Our findings can be summarized as follows:

- We propose a new momentum decay rule, dubbed as DEMON. DEMON is motivated by decaying the total contribution of a gradient to all future updates, with limited additional computation.
- Across 28 relevant settings, DEMON achieves the highest ratio of Top-1 and Top-3 finishes: 39% and 85%, respectively. See Table 1. These ratios nearly double those of the second-placed cosine learning rate decay schedule, which achieves 17% and 60%, respectively. In addition to outperforming other popular schedule such as the learning rate step schedule, linear schedule, and OneCycle, DEMON also outperforms all other momentum schedules that were considered.
- We observe improved robustness to hyperparameter tuning for DEMON relative to the popular learning rate step schedule.

Experiments are provided on various datasets—including MNIST, FMNIST, CIFAR-10, CIFAR-100, STL-10, Tiny ImageNet, Penn Treebank (PTB), GLUE benchmark [68]; and networks—including Convolutional Networks (CNN) with Residual architecture (ResNet) [23] (Wide ResNet) [79], Non-Residual architecture (VGG-16) [60], Recurrent Neural Networks (RNN) with Long Short-Term Memory architecture (LSTM) [26], Variational AutoEncoders (VAE) [33], Capsule Network [53], Noise Conditional Score Network (NCSN) [65], and BERT [16].

2 PRELIMINARIES

SGDM. Let $\theta_t \in \mathbb{R}^p$ be the parameters of the network at time step t , where $\eta \in \mathbb{R}$ is the learning rate, and g_t is the stochastic gradient w.r.t. θ_t for empirical loss $\mathcal{L}(\cdot)$. SGDM is parameterized by $\beta \in \mathbb{R}$, the momentum coefficient, and follows the recursion:

$$\theta_{t+1} = \theta_t + \eta v_t, \quad v_t = \beta v_{t-1} - g_t,$$

where $v_t \in \mathbb{R}^p$ accumulates momentum. Observe that for $\beta = 0$, the above recursion is equivalent to SGD. Common values for β are closer to one, with $\beta = 0.9$ the most used value [52].

Adaptive gradient descent methods. These algorithms utilize current and past gradients to design preconditioning matrices that better approximate the local curvature of $\mathcal{L}(\cdot)$ [18, 25]. Adam [32] uses a decaying average of past gradients, as in $\mathcal{E}_{t+1}^g = \beta_1 \cdot \mathcal{E}_t^g + (1 - \beta_1) \cdot g_t$, as well as a decaying average of squared gradients, as in $\mathcal{E}_{t+1}^{g \circ g} = \beta_2 \cdot \mathcal{E}_t^{g \circ g} + (1 - \beta_2) \cdot (g_t \circ g_t)$, leading to the recursion:¹

$$\theta_{t+1,i} = \theta_{t,i} - \frac{\eta}{\sqrt{\mathcal{E}_{t+1,i}^{g \circ g} + \varepsilon}} \cdot \mathcal{E}_{t+1,i}^g, \quad \forall t,$$

where usually $\beta_1 = 0.9$ and $\beta_2 = 0.999$.

3 DEMON: DECAYING MOMENTUM ALGORITHM

DEMON is motivated by learning rate decay models which reduce the impact of a gradient to current and future updates. By decaying momentum, we decay the total contribution of a gradient to all future updates. *Our goal here is to present a concrete, effective, and easy-to-use momentum decay procedure, which we show in the*

¹For clarity, we will skip the bias correction step in this description of Adam; see [32].

experimental section. The key component is the momentum decay schedule:

$$\beta_t = \beta_{\text{init}} \cdot \frac{(1 - \frac{t}{T})}{(1 - \beta_{\text{init}}) + \beta_{\text{init}}(1 - \frac{t}{T})}. \quad (1)$$

Above, the fraction $(1 - t/T)$ refers to the proportion of iterations remaining. Fig. 1 presents a visualization of the proposed momentum decay rule and other common schedules. The interpretation of this rule comes from the following argument: Assume fixed momentum parameter $\beta_t \equiv \beta$; e.g., $\beta = 0.9$, as literature dictates. For our discussion, we will use the SGDM recursion. We know that $v_0 = 0$, and $v_t = \beta v_{t-1} - g_t$. Then, the main recursion can be unrolled into:

$$\begin{aligned} \theta_{t+1} &= \theta_t - \eta g_t - \eta \beta g_{t-1} - \eta \beta^2 g_{t-2} + \eta \beta^3 v_{t-2} \\ &= \dots = \theta_t - \eta g_t - \eta \cdot \sum_{i=1}^t (\beta^i \cdot g_{t-i}) \end{aligned}$$

Interpreting the above recursion, *a particular gradient term g_t contributes a total of $\eta \sum_i \beta^i$ of its “energy” to all future gradient updates.* Moreover, for an asymptotically large number of iterations, we know that β contributes on up to $t - 1$ terms. Then, $\sum_{i=1}^{\infty} \beta^i = \beta \sum_{i=0}^{\infty} \beta^i = \beta / (1 - \beta)$. Thus, in our quest for a simple momentum decay schedule, it is natural to consider a scheme where the cumulative momentum is decayed to 0. Let β_{init} be the initial β ; then at the current step t with a total of T steps, we design the decay routine such that: $\beta / (1 - \beta) = (1 - t/T) \beta_{\text{init}} / (1 - \beta_{\text{init}})$. This leads to (1). Although β changes in subsequent iterations, this is typically a very close approximation because $\beta^i \beta^{i+1} \dots \beta^t$ for a particular g^i diminishes much faster than β changes.

Formal intuition. Conceptually, Demon takes advantage of momentum for speed-up in the early phases of training, but decays momentum throughout training. This prevents neural network weights from growing too quickly. Constraining weights has been recently studied and shown to be key for optimal performance. In particular, it is demonstrated theoretically and empirically in [24] that plain use of momentum leads to suboptimal performance. It is important to stabilize the growth of the weights across training.

Formally, a function f is scale invariant if $f(cx) = f(x)$ for constant $c > 0$. Let the function $\text{Norm}(\cdot)$ be defined as $\text{Norm}_s(x) = (x - \mu_s(x)) / \sigma_s(x)$, where s is a subset of the dimensions of x , μ_s is the mean for those dimensions, and σ_s the standard deviation. $\text{Norm}(\cdot)$ is scale invariant, and includes cases such as Batch Norm [24]. Concretely, $\text{Norm}(\theta^T x) = \text{Norm}((c\theta)^T x)$. With adaptive β_t on iteration t , we extend the norm growth lemma in [24] as follows:

LEMMA 1. *For scale invariant θ given by momentum SGD, the following equality holds true:*

$$\|\theta_{t+1}\|_2^2 = \|\theta_t\|_2^2 + \eta^2 \|v_t\|_2^2 + 2\eta^2 \sum_{i=0}^{t-1} \beta_i \beta_{i+1} \dots \beta_{t-1} \|v_i\|_2^2$$

Since the latter term grows increasingly larger, Demon decays the momentum to curb its growth, and therefore reduces the norm growth of the parameters, leading to improved performance [24]. The extension is trivial and the proof is omitted.

Connection to previous algorithms. DEMON introduces an implicit discount factor. The main recursions of the algorithm resemble those of standard machine learning algorithms. E.g., for $\beta_t = \beta = 0.9$ we obtain SGD with momentum, and for $\beta = 0$ we

obtain plain SGD in Algorithm 1; in Algorithm 2, for $\beta_1 = 0.9$ with a slight adjustment of learning rate we obtain Adam, while for $\beta_1 = 0$ we obtain a non-accumulative AdaGrad algorithm. We choose to apply DEMON to a slightly adjusted Adam to isolate the effect of the momentum parameter, since the momentum parameter adjusts the magnitude of the current gradient as well in vanilla Adam.

Efficiency. DEMON requires only limited extra overhead and computation in comparison to the vanilla counterparts for the computation of β_t . Implementation is simply 1-2 lines of code.

```
p_t = (iters - t) / iters
beta_t = beta1 * (p_t / (1 - beta1 + beta1 * p_t))
```

Convergence analysis. *We provide convergence proof for DEMON SGDM in the convex setting, by bounding auxiliary function sequences [20]. For an objective function f which is convex, continuously differentiable, its gradient $\nabla f(\cdot)$ is Lipschitz continuous with constant L , our goal is to show that $f(\bar{\theta}_T)$ converges to the optimum f^* with decreasing momentum, where $\bar{\theta}_T$ is the average of θ_t for $t = 1, \dots, T$, following [20]. Our following theorem holds for a constant learning rate and β_t decaying with t .*

THEOREM 1. *Assume that f is convex, continuously differentiable, its gradient $\nabla f(\cdot)$ is Lipschitz continuous with constant L , with a decreasing momentum, but constant step size, as in: $\beta_t = \frac{1}{t} \cdot \frac{t+1}{t+2}$, $\alpha \in (0, \frac{2}{3L})$. We consider the SGDM iteration in non-stochastic settings, where: $\theta_{t+1} = \theta_t - \alpha \nabla f(\theta_t) + \beta_t (\theta_t - \theta_{t-1})$. Then, the sequence $\{\theta_t\}_{t=1}^T$ generated by the SGDM iteration, with decreasing momentum, satisfies:*

$$f(\bar{\theta}_T) - f^* \leq \frac{\|\theta_1 - \theta^*\|^2}{T} \left(\frac{3}{4}L + \frac{1}{2\alpha} \right),$$

where $\bar{\theta}_T$ is the Cesaro average of the iterates: $\bar{\theta}_T = \frac{1}{T} \sum_{t=1}^T \theta_t$.

Proof. Let $\beta_t = \frac{1}{t} \cdot \frac{t+1}{t+2}$ and $p_t = \frac{1}{t} (\theta_t - \theta_{t-1})$. We consider the SGDM iteration in non-stochastic settings, where $\theta_{t+1} = \theta_t - \alpha \nabla f(\theta_t) + \beta_t (\theta_t - \theta_{t-1})$. Using the definition of p_t above, one can easily prove that:

$$\theta_{t+1} + p_{t+1} = \left(1 + \frac{1}{t+1}\right) \theta_{t+1} - \frac{1}{t+1} \theta_t = \theta_t + p_t - \frac{\alpha(t+2)}{t+1} \nabla f(\theta_t).$$

Using this expression, we will analyze the term $\|\theta_{t+1} + p_{t+1} - \theta^*\|_2$:

$$\begin{aligned} \|\theta_{t+1} + p_{t+1} - \theta^*\|^2 &= \|\theta_t + p_t - \theta^*\|^2 \\ &\quad - \frac{2\alpha(t+2)}{t+1} \langle \theta_t + p_t - \theta^*, \nabla f(\theta_t) \rangle \\ &\quad + \left(\frac{\alpha(t+2)}{t+1} \right)^2 \cdot \|\nabla f(\theta_t)\|^2 \\ &= \|\theta_t + p_t - \theta^*\|^2 - \frac{2\alpha(t+2)}{t(t+1)} \langle \theta_t - \theta_{t-1}, \nabla f(\theta_t) \rangle \\ &\quad - \frac{2\alpha(t+2)}{t+1} \langle \theta_t - \theta^*, \nabla f(\theta_t) \rangle \\ &\quad + \left(\frac{\alpha(t+2)}{t+1} \right)^2 \cdot \|\nabla f(\theta_t)\|^2 \end{aligned}$$

Since f is convex, continuously differentiable, its gradient is Lipschitz continuous with constant L , then

$$\frac{1}{L} \|\nabla f(\theta_t)\|^2 \leq \langle \theta_t - \theta^*, \nabla f(\theta_t) \rangle, \quad (2)$$

$$f(\theta_t) - f^* + \frac{1}{2L} \|\nabla f(\theta_t)\|^2 \leq \langle \theta_t - \theta^*, \nabla f(\theta_t) \rangle, \quad (3)$$

$$f(\theta_t) - f(\theta_{t-1}) \leq \langle \theta_t - \theta_{t-1}, \nabla f(\theta_t) \rangle. \quad (4)$$

Substituting the above inequalities leads to

$$\begin{aligned} \|\theta_{t+1} + p_{t+1} - \theta^*\|^2 &\leq \|\theta_t + p_t - \theta^*\|^2 - \frac{2\alpha(t+2)}{t(t+1)} (f(\theta_t) - f(\theta_{t-1})) \\ &\quad - 2\alpha \frac{(1-\lambda)(t+2)}{L(t+1)} \cdot \|\nabla f(\theta_t)\|^2 \\ &\quad - 2\alpha\lambda \frac{t+2}{t+1} (f(\theta_t) - f^*) \\ &\quad - \left(\alpha \frac{\lambda(t+2)}{L(t+1)} \right) \cdot \|\nabla f(\theta_t)\|^2 \\ &\quad + \left(\frac{\alpha(t+2)}{t+1} \right)^2 \cdot \|\nabla f(\theta_t)\|^2 \end{aligned}$$

where $\lambda \in (0, 1]$ is a parameter weighting (2) and (3). Grouping together terms yields

$$\begin{aligned} &\left(\frac{2\alpha(t+2)}{t(t+1)} + \frac{2\alpha\lambda(t+2)}{t+1} \right) (f(\theta_t) - f^*) + \|\theta_{t+1} + p_{t+1} - \theta^*\|^2 \leq \\ &\quad \frac{2\alpha(t+2)}{t(t+1)} (f(\theta_{t-1}) - f^*) + \|\theta_t + p_t - \theta^*\|^2 \\ &\quad + \frac{\alpha(t+2)}{t+1} \left(\frac{\alpha(t+2)}{t+1} - \frac{2(1-\lambda)}{L} - \frac{\lambda}{L} \right) \|\nabla f(\theta_t)\|^2. \end{aligned}$$

The last term is non-positive when $\alpha \in [0, \frac{t+1}{t+2}(\frac{2-\lambda}{L})]$ so it can be dropped. Summing over $t = 1, \dots, T$ yields

$$\begin{aligned} &2\alpha\lambda \sum_{t=1}^T \frac{t+2}{t+1} (f(\theta_t) - f^*) \\ &+ \sum_{t=1}^T \left(\frac{2\alpha(t+2)}{t(t+1)} (f(\theta_t) - f^*) + \|\theta_{t+1} + p_{t+1} - \theta^*\|^2 \right) \leq \\ &\sum_{t=1}^T \left(\frac{2\alpha(t+2)}{t(t+1)} (f(\theta_{t-1}) - f^*) + \|\theta_t + p_t - \theta^*\|^2 \right), \end{aligned}$$

implying that:

$$2\alpha\lambda \sum_{t=1}^T \frac{t+2}{t+1} (f(\theta_t) - f^*) \leq 3\alpha(f(\theta_1) - f^*) + \|\theta_1 - \theta^*\|^2.$$

Since: $2\alpha\lambda \sum_{t=1}^T (f(\theta_t) - f^*) \leq 2\alpha\lambda \sum_{t=1}^T \frac{t+2}{t+1} (f(\theta_t) - f^*) \leq 3\alpha\lambda \sum_{t=1}^T (f(\theta_t) - f^*)$, we further have:

$$3\alpha\lambda \sum_{t=1}^T (f(\theta_t) - f^*) \leq \frac{3}{2} \left(3\alpha(f(\theta_1) - f^*) + \|\theta_1 - \theta^*\|^2 \right).$$

Due to the convexity of f : $f(\bar{\theta}_t) \leq \frac{1}{T} \sum_{t=1}^T f(\theta_t)$, observe that

$$\begin{aligned} f(\bar{\theta}_T) - f^* &\leq \frac{1}{T} \sum_{t=1}^T (f(\theta_t) - f^*) \leq \\ &\frac{1}{3\alpha\lambda T} \left(\frac{9}{2}\alpha(f(\theta_1) - f^*) + \frac{3}{2}\|\theta_1 - \theta^*\|^2 \right). \end{aligned}$$

Since $f(\theta_1) - f^* \leq \frac{L}{2}\|\theta_1 - \theta^*\|^2$ by Lipschitz continuous gradients, setting $\lambda = 1$ and observing $(t+1)/(t+2) \geq 2/3$ gives the result.

For DEMON Adam, we observe it lies within the definition of Generic Adam in [82], and inherits the non-convex results. Namely, to restate the theorem [82]:

THEOREM 2. *Assuming $\tau \in \{1, 2, \dots, T\}$ is an index over T iterations, Demon + Adam satisfies:*

$$\mathbb{E}[\|\nabla f(x_\tau)\|_2^{4/3}]^{3/2} \leq \frac{C + C' \sum_t \alpha_t \sqrt{1 - \theta_t}}{\alpha_T \cdot T} = O\left(\frac{1}{T}\right),$$

where C, C' are constants, α_t are step sizes, θ_t are the parameters related to the diagonal Hessian approximation of Adam's preconditioner, and $\beta_t < 1$, as is the case for Demon technique.

Moreover, one can remove the expectation requirement above, and have the same result hold deterministically with some probability $1 - \delta^{2/3}$:

$$\|\nabla f(x_\tau)\|_2^2 \leq \frac{C + C' \sum_t \alpha_t \sqrt{1 - \theta_t}}{\delta \cdot \alpha_T \cdot T} = O\left(\frac{1}{T}\right).$$

To achieve the above, the assumptions are lower-bounded function f , L -smoothness, and standard assumptions on gradients. Regarding the parameters, momentum β_t has to satisfy $0 \leq \beta_t \leq \beta < 1$, for some β : this is exactly the setting of Demon, where β is the initial value of the momentum, and β_t decreases to zero. Our work is an exact instance of decreasing momentum that leads to empirical improvements compared to previous work; to the best of our knowledge, no other paper has considered a specific decreasing schedule for momentum that is at the same time almost "hyperparameter-free".

Practical suggestions. We advocate for decaying momentum from β_{init} at $t = 0$, to 0 at $t = T$ as a general rule, which is the setting we use for all DEMON experiments in this paper.

4 RELATED WORK

Numerous techniques exist for automatic hyperparameter tuning. Adaptive methods, such as AdaGrad [18], AdaDelta [80], RMSprop [25], and Adam [32], are most widely used. Interest in closing the generalization difference between adaptive methods and SGDM led to AMSGrad [50], which uses the maximum of the exponential moving average of squared gradients, QHAdam [41], a variant of QHM that recovers a variety of optimization algorithms, AdamW [38], which decouples weight decay in Adam, and Padam [10], which lowers the exponent of the second moment. YellowFin [81] is a learning rate and momentum adaptive method motivated by a quadratic model analysis and robustness insights. In the non-convex setting, STORM [13] uses a variant of momentum for variance reduction.

The convergence of momentum methods has been heavily explored both empirically and theoretically [15, 31, 71, 72, 74]. [67] explored momentum schedules, even increasing momentum during training, inspired by Nesterov's routines for convex optimization. [63] scales the batch size to create associated changes in learning rate and momentum. [62] introduces cycles of simultaneously increasing learning rate and decreasing momentum followed by simultaneously decreasing learning rate and increasing momentum. Some work adapts the momentum to reduce oscillations during training [46] and explores integration of momentum into well-conditioned convex problems [66]. Another approach is to combine several momentum vectors with different β values [40]. In another work, gradient staleness in variance reduction methods is addressed with gradient transport [5]. We are aware of the theoretical work of

[78] that proves, under certain conditions, SGDM is equivalent to SGD with a rescaled learning rate, but our experiments in the deep learning setting show slightly different behavior. Understanding this discrepancy is an exciting direction of research.

Smaller values of β have been employed for Generative Adversarial Networks (GANs), and recent developments in game dynamics [22] show a negative momentum is helpful.

5 EXPERIMENTS

Well-known experiments in the literature are selected for comparison (e.g., ResNets, LSTMs, and BERT). *Training models like GPT-2/3 from scratch is not feasible, and we instead focus on providing a wide number of experiments and baselines.* For each setting, we use varying numbers of epochs to demonstrate effectiveness. Experiments with different numbers of epochs are standalone experiments with independently-tuned hyperparameters. All settings are summarized in Table 2 and comprehensively detailed in Appendix A.

Table 2: Summary of experimental settings.

Experiment short name	Model	Dataset
RN20-CIFAR10	ResNet20	CIFAR10
RN56-TINYIMAGENET	ResNet56	Tiny ImageNet
VGG16-CIFAR100	VGG-16	CIFAR100
WRN-STL10	Wide ResNet 16-8	STL10
LSTM-PTB	LSTM RNN	Penn TreeBank
VAE-MNIST	VAE	MNIST
NCSN-CIFAR10	NCSN	CIFAR10
CAPS-FMNIST	Capsnet	FMNIST
BERT _{BASE} -GLUE	BERT (Pre-trained)	GLUE (9 tasks)

We note that we have implemented setups that use the standard ImageNet dataset as input. However, we did not observe any results worth noting between learning rate step decay and DEMON. In particular, using a ResNet-50, comparable performance to state of the art is achieved using most algorithms under consideration. ImageNet results are often not indicative of generalizability, see [58], and this highlights that a breadth of experiments is more important.

We consider the following schedules, where we tune both the learning rate in multiples of 3, the momentum $\in [0.9, 0.95, 0.97]$, and weight decay, in addition to the other hyperparameters specialized to the particular schedule. The cost refers to if there are any other hyperparameters to tune that are specialized to the schedule.

- *No schedule*: Self-explanatory (**1× cost**).
- *Step schedule*: One of the most common kind of schedules (at this moment) for achieving state-of-the-art results in the literature [28, 29, 37, 69, 79]. We attempt decay schedules including 0.1× at 50% and 75% of total epochs; 0.1× at 25%, 50%, 75%; 0.1× at 33% and 66%; 0.1× at 10%, 25%, 50%, 75% (**4× cost**).
- *Cosine schedule*[39]: Follows the smooth schedule of $\gamma_t = \gamma_{min} + 0.5 \cdot (\gamma_{max} - \gamma_{min}) (1 + \cos(\pi t/T))$. γ can be the learning rate or the momentum. We consider $\gamma_{min} = 0$ to achieve (**1× cost**).
- *OneCycle*[62]: This scheme roughly follows increasing learning rate linearly from 0.1η to η and back to 0.1η , while simultaneously decreasing momentum linearly from β_{max} to β_{min} and back to

β_{max} . For the momentum values, we consider the pairs [(0.95, 0.85), (0.9, 0.85), (0.95, 0.9)]. For the momentum variant, we simply consider the momentum component of OneCycle (**1× cost**).

- *Linear schedule*: Decreases the hyperparameter from the initial value to 0 across epochs (**1× cost**).
- *Exponential schedule*[1]: Follows the smooth schedule of $\gamma_t = \gamma \cdot e^{kt}$. We tune k from a reasonable starting point, $-0.05 \cdot (100/T)$ which is a scaled version of the curve in Figure 1 (i.e., plotted for 100 iterations in multiples of 2) (**~4× cost**).
- *Decay on Plateau*[1]: Commonly used in practice where the learning rate is multiplied by a factor if validation loss stops improving for a certain number of epochs (patience). We tune the patience in multiples of 5, and multiply the learning rate by 0.1 (**~5× cost**).
- **DEMON**: This paper. The schedule follows Algorithm 1 and decays to 0 at the end of training (**1× cost**).

We apply these schedules to SGDM and Adam, focusing on the performance of different schedules. *The overall tuning budget for DEMON SGDM/Adam is generally equal to or less than that of SGDM/Adam with its relevant possible schedules.*

5.1 Decreasing the need for tuning

We demonstrate the hyperparameter robustness of DEMON SGDM and DEMON Adam relative to SGDM with learning rate step schedule and Adam. In Fig. 2, validation accuracy is displayed for a grid search over learning rate and momentum. For SGDM, results are obtained with the highest-performing learning rate schedule. The heatmaps display optimal performance of each optimizer over the full range of possible hyperparameters.

WRN-STL10-DEMONSGDM yields a significantly larger band of lighter color, indicating better performance for a wide range of hyperparameters. For every learning rate-momentum pair, we observe a lighter color for DEMON SGDM relative to SGDM. Concretely, SGDM has roughly one configuration per column with < 22% generalization error, while DEMON SGDM has five.

On VGG16-CIFAR100-DEMONSGDM, a larger band of low generalization error exists compared to SGDM. There also appears to be a slight shift in optimal parameters. Concretely, DEMON SGDM has almost three times the number of configurations with generalization error < 31%.

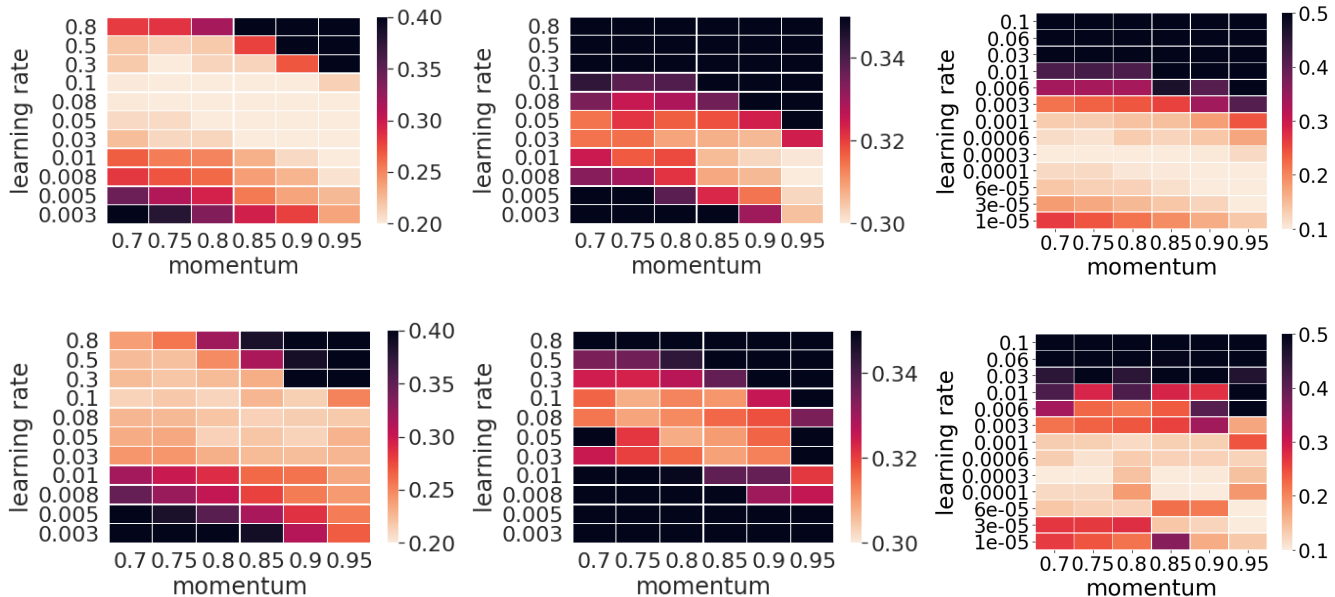
On RN20-CIFAR10, DEMON Adam demonstrates its improved hyperparameter robustness relative to Adam. The generalization errors achieved with Adam fluctuate significantly, yielding optimal performance with only a few hyperparameter settings. In contrast, DEMON Adam yields a wide band of high performance across hyperparameters.

These results suggest that both DEMON Adam and DEMON SGDM are less sensitive to hyperparameter tuning than their learning rate step schedule counterparts, whilst attaining competitive error. This is critical to the use of DEMON in practice, as DEMON can yield high performance with minimal tuning. The performance of DEMON is high and stable across a wide range of hyperparameters near the default.

5.2 Results

For benchmarking purposes, we also include some other baselines where the learning rate and/or momentum are automatically

Figure 2: Left to right: Error rate for WRN-STL10-DEMONSGDM (top) and WRN-STL10-SGDM (bottom) for 50 epochs, error rate for VGG16-CIFAR100-DEMONSGDM (top) and VGG16-CIFAR100-SGDM (bottom) for 100 epochs, and error rate for RN20-CIFAR10-DEMONAdam (top) and RN20-CIFAR10-Adam (bottom) for 100 epochs. Light-colored patches indicate better performance.



adapted. These include Quasi Hyperbolic Adam (QHAdam) [41], Quasi Hyperbolic Momentum (QHM) [41], AMSGrad [50], AdamW [38], YellowFin [81], Aggregated Momentum (AggMo) [40]. Quasi Hyperbolic methods are capable of recovering Accelerated SGD [30], Nesterov Accelerated Gradient [45], Synthesized Nesterov Variants [35], and others, thus covering more algorithms than those present. However, these methods are included primarily for reference, and the major focus of this work is on the schedules describe at the beginning of Section 5. *We emphasize that DEMON can be combined with any momentum method. We present results with SGDM and Adam due to their wide usage.*

Mainline results We summarize the results of all relevant settings in Table 1. Out of the 28 relevant settings in this paper, DEMON achieves the highest percentage of Top-1 and Top-3 finishes, with 39% and 85% respectively. Other momentum decay schedules are not competitive, likely due to being overly aggressive. Learning rate step schedule, linear schedule, and cosine schedule perform comparably; however, the different learning rate schedulers do not always yield comparable performance across settings. For example, linear learning rate decay performs exceptionally well in the ResNet settings, but closer to average on other settings. Such results indicate that the decay schedule, for learning rate or momentum, is an additional hyperparameter that must be tuned. Even though Decay On Plateau and Exponential Decay are implemented in most popular frameworks as empirical alternatives, they perform poorly when the total number of epochs are predefined. DEMON is the most consistent across a wide range of settings, with by far the highest Top-3 performance.

Residual Networks (RN20-CIFAR10). We train a ResNet20 [23] model on the CIFAR-10 dataset. We emphasize that ResNet20 is commonly conflated with the more expressive ResNet18, which achieves different performance. This is an important setting to evaluate because ResNets remain one of the most popular computer vision architectures in both academia and industry, achieving reasonable performance with less risk of overfitting to the test set [58]. The other ResNet settings include WRN-STL10, a Wide Residual 16-8 model [79] on STL-10 that has significantly fewer, higher resolution images in comparison to CIFAR, and RN56-TINYIMAGENET, a ResNet56 model on the Tiny ImageNet dataset. Due to limited resources, the runs of RN56-TINYIMAGENET are conducted to supplement the other settings. See Table 3 for results.

In sum, the other momentum decay schedules do not perform well, likely due to the overly aggressive momentum decay. The momentum component of OneCycle, when used in isolation, appears to destabilize training, leading in some cases to performance worse than the vanilla counterpart. Whilst traditionally the learning rate step schedule is the most popular and often used to achieve state-of-the-art results in computer vision, this schedule has no clear advantage over the learning rate cosine schedule, the learning rate linear schedule, or DEMON. DEMON has the strongest performance, even outperforming methods that automatically tune the momentum parameter.

Non-Residual Convolutional Network (VGG16-CIFAR100). We train an adjusted VGG-16 model [60] on the CIFAR-100 dataset. Previous observations from the ResNet settings continue to hold, where other momentum decay methods are not competitive. Again, the learning rate step schedule does not appear to provide any

Table 3: RN20-CIFAR10, WRN-STL10 and RN56-TINYIMAGENET generalization error. The number of epochs was predefined before the execution of the algorithms. Red indicates Top-1 performance, bold is Top-3, ignoring non SGDM and Adam optimizers.

	ResNet 20			Wide ResNet 16-8			ResNet 56	
	75 epochs	150 epochs	300 epochs	50 epochs	100 epochs	300 epochs		
SGDM								
+ LR Step Schedule	8.82 ± .25	8.43 ± .07	7.32 ± .14	22.42 ± .56	17.20 ± .35	14.51 ± .26	45.98 ± .23	41.66 ± .10
+ LR Cosine Schedule	8.80 ± .08	8.10 ± .13	7.78 ± .14	20.03 ± .26	17.02 ± .24	14.66 ± .25	-	-
+ OneCycle	10.83 ± .25	9.23 ± .19	8.42 ± .12	21.67 ± .27	19.69 ± .21	19.00 ± .42	-	-
+ LR Linear Schedule	9.03 ± .24	8.15 ± .12	7.62 ± .12	19.54 ± .20	17.39 ± .24	14.58 ± .18	-	-
+ LR Decay on Plateau	9.05 ± .07	8.26 ± .07	7.97 ± .14	21.05 ± .27	17.83 ± .39	15.16 ± .36	-	-
+ LR Exp decay	9.55 ± .09	9.20 ± .13	7.82 ± .05	22.65 ± .49	20.60 ± .21	15.85 ± .28	-	-
+ OneCycle Momentum	15.61 ± .39	14.02 ± .13	13.35 ± .58	29.34 ± .78	23.20 ± .39	25.42 ± .47	-	-
+ Cosine Momentum	13.57 ± .20	11.23 ± .22	10.87 ± .03	24.12 ± .34	21.66 ± .37	16.29 ± .26	-	-
+ Linear Momentum	12.31 ± .14	10.26 ± .16	10.63 ± .31	25.13 ± .28	22.74 ± .78	17.92 ± .41	-	-
+ Exp Momentum decay	14.96 ± .19	12.98 ± .15	12.35 ± .11	24.01 ± .20	19.35 ± .29	17.56 ± .21	-	-
AggMo + LR Step	8.71 ± .24	7.93 ± .15	7.62 ± .03	21.37 ± .32	17.15 ± .35	14.49 ± .26	-	-
QHM + LR Step	8.72 ± .14	7.95 ± .17	7.67 ± .10	21.75 ± .31	18.21 ± .48	14.44 ± .23	-	-
DEMON SGDM	8.56 ± .10	8.21 ± .18	7.59 ± .12	20.23 ± .31	16.19 ± .23	14.44 ± .53	44.87 ± .15	40.85 ± .01
Adam	13.63 ± .22	11.90 ± .06	11.94 ± .06	23.35 ± .20	19.63 ± .26	18.65 ± .07	57.56 ± 1.50	50.89 ± .59
+ LR Step Schedule	10.47 ± .10	8.75 ± .17	8.55 ± .05	23.85 ± .07	19.63 ± .33	18.29 ± .10	-	-
+ LR Cosine Schedule	9.56 ± .12	9.15 ± .12	8.93 ± .07	22.85 ± .47	21.47 ± .31	19.08 ± .36	-	-
+ OneCycle	10.33 ± .20	9.87 ± .12	9.03 ± .18	20.02 ± .19	19.21 ± .28	19.03 ± .43	-	-
+ LR Linear Schedule	9.25 ± .12	9.20 ± .22	8.89 ± .05	21.70 ± .11	21.53 ± .44	17.85 ± .15	-	-
+ LR Decay on Plateau	9.71 ± .39	8.92 ± .18	8.80 ± .11	22.77 ± .33	19.91 ± .45	19.61 ± .56	-	-
+ LR Exp decay	10.48 ± .15	9.24 ± .16	8.53 ± .07	23.30 ± .39	20.70 ± .50	19.63 ± .24	-	-
+ OneCycle Momentum	20.05 ± .91	15.60 ± .69	14.85 ± .50	24.61 ± .54	23.39 ± .39	23.54 ± .38	-	-
+ Cosine Momentum	11.08 ± .11	10.63 ± .20	10.64 ± .30	25.76 ± .22	23.58 ± .02	20.10 ± .15	-	-
+ Linear Momentum	11.91 ± .18	11.48 ± .13	11.09 ± .12	24.36 ± .31	21.93 ± .23	21.81 ± .36	-	-
+ Exp Momentum decay	15.18 ± .10	12.08 ± .16	10.63 ± .12	28.90 ± .21	25.28 ± .31	22.90 ± .41	-	-
AMSGrad	13.43 ± .14	11.83 ± .12	10.48 ± .12	21.73 ± .25	19.35 ± .20	18.21 ± .18	-	-
AdamW	12.46 ± .52	11.38 ± .21	10.50 ± .17	20.39 ± .62	18.55 ± .23	17.00 ± .41	-	-
QHAdam	15.55 ± .25	13.78 ± .08	13.36 ± .11	21.25 ± .22	19.81 ± .18	18.52 ± .25	-	-
YellowFin	13.66 ± .34	12.13 ± .41	11.39 ± .16	22.55 ± .14	20.68 ± .04	18.56 ± .33	-	-
DEMON Adam	9.68 ± .07	8.90 ± .18	8.50 ± .12	20.95 ± .23	19.50 ± .32	18.62 ± .41	48.92 ± .03	45.72 ± .31



Figure 4: Randomly selected CIFAR10 images generated with NCSN. Left: Real CIFAR10 images. Middle: Adam. Right: DEMON Adam.

advantage over the cosine schedule, linear schedule, or DEMON, the latter of which performs the best. See Table 4.

LSTM (PTB-LSTM). We apply an LSTM [26] architecture to the language modeling task, which has notoriously sharp gradient distributions (e.g., rare words). We use the official TensorFlow v1 implementation for PTB - LSTM. OneCycle Momentum is adjusted to decay to 0 and back since this setting typically requires low

momentum to train well. Such characteristically low momentum makes this task a difficult test case for momentum decay methods, as momentum seems to have less impact on performance relative to other settings. However, more momentum values are also swept to achieve the reported perplexity. As a whole, smooth decay methods do not perform comparably to step decay methods on this task. DEMON is surprisingly competitive and is the only momentum

Table 4: VGG16-CIFAR100 generalization error, LSTM-PTB generalization perplexity, VAE-MNIST generalization loss, and CAPS-FMNIST generalization error. The number of epochs was predefined before the execution of the algorithms. Red indicates Top-1 performance, bold is Top-3, ignoring non SGDM and Adam optimizers.

	VGG-16		LSTM		VAE		CAPSNET	
	150 epochs	300 epochs	25 epochs	39 epochs	50 epochs	100 epochs	50 epochs	100 epochs
SGDM								
+ LR Step Schedule	30.09 ± .32	27.83 ± .30	81.67 ± .21	82.02 ± .13	140.28 ± .51	137.70 ± .93	-	-
+ LR Cosine Schedule	28.63 ± .11	27.84 ± .12	81.64 ± .37	83.23 ± .06	139.15 ± .26	136.69 ± .27	-	-
+ OneCycle	30.10 ± .34	29.09 ± .12	90.03 ± .39	91.19 ± .01	139.79 ± .66	137.20 ± .06	-	-
+ LR Linear Schedule	29.10 ± .34	28.26 ± .08	96.27 ± .09	98.79 ± .02	148.00 ± .48	141.72 ± .48	-	-
+ LR Decay on Plateau	30.65 ± .31	29.74 ± .43	81.55 ± .24	81.82 ± .07	140.51 ± .73	139.54 ± .34	-	-
+ LR Exp decay	29.51 ± .22	28.47 ± .18	84.20 ± .08	83.49 ± .03	154.31 ± .43	145.83 ± .48	-	-
+ OneCycle Momentum	35.86 ± .25	35.34 ± .30	87.14 ± .27	91.93 ± 1.03	144.90 ± .61	142.63 ± .25	-	-
+ Cosine Momentum	32.73 ± .07	30.99 ± .11	88.33 ± .92	90.02 ± .10	145.13 ± .85	140.14 ± .81	-	-
+ Linear Momentum	31.61 ± .29	31.23 ± .26	90.02 ± .51	93.06 ± .29	145.33 ± .13	139.83 ± .14	-	-
+ Exp Momentum decay	34.50 ± .23	32.83 ± .13	86.39 ± .20	89.45 ± .63	150.54 ± 1.07	156.95 ± .47	-	-
AggMo + LR Step	30.75 ± .55	28.64 ± .45	83.15 ± .12	83.43 ± .17	139.49 ± .99	136.56 ± .28	-	-
QHM + LR Step	29.93 ± .13	29.01 ± .54	88.75 ± .23	88.42 ± .10	142.47 ± .50	137.97 ± .54	-	-
DEMON SGDM	28.67 ± .11	27.69 ± .11	82.66 ± .05	84.84 ± .22	138.29 ± .08	136.55 ± .64	-	-
Adam	33.62 ± .11	31.09 ± .09	109.48 ± .36	116.26 ± .10	136.28 ± .18	134.64 ± .14	9.27 ± .08	9.25 ± .11
+ LR Step Schedule	29.40 ± .22	27.75 ± .15	98.79 ± .05	99.69 ± .03	136.62 ± .30	134.14 ± .56	8.90 ± .03	8.98 ± .05
+ LR Cosine Schedule	29.68 ± .17	28.08 ± .10	97.70 ± .07	100.56 ± .27	134.73 ± .04	133.25 ± .26	9.16 ± .07	9.75 ± .10
+ OneCycle	29.83 ± .29	29.58 ± .18	112.32 ± .10	117.31 ± .11	134.67 ± .55	133.27 ± .07	9.21 ± .04	8.88 ± .04
+ LR Linear Schedule	29.30 ± .18	28.65 ± .10	111.10 ± .83	115.24 ± .10	134.71 ± .25	134.00 ± .49	8.90 ± .10	8.90 ± .04
+ LR Decay on Plateau	29.03 ± .10	28.67 ± .19	99.65 ± .18	101.46 ± .22	135.68 ± .59	134.10 ± .21	9.10 ± .09	9.12 ± .07
+ LR Exp decay	29.53 ± .12	28.83 ± .08	103.50 ± .41	103.09 ± .10	135.19 ± .43	134.05 ± .16	8.80 ± .07	8.72 ± .08
+ OneCycle Momentum	36.98 ± .29	32.96 ± .37	106.86 ± .66	108.77 ± .08	138.16 ± .35	136.68 ± .47	9.79 ± .09	9.95 ± .08
+ Cosine Momentum	31.65 ± .16	30.54 ± .16	105.78 ± .04	106.01 ± .09	135.62 ± .38	134.02 ± .10	9.13 ± .06	8.82 ± .10
+ Linear Momentum	32.28 ± .13	29.65 ± .11	106.38 ± .49	114.24 ± .14	136.24 ± .87	135.00 ± .51	9.12 ± .08	9.03 ± .04
+ Exp Momentum decay	32.05 ± .14	30.63 ± .14	104.32 ± .26	115.87 ± .12	136.67 ± .56	136.05 ± .11	9.00 ± .07	9.22 ± .08
AMSGrad	34.46 ± .21	31.62 ± .12	103.12 ± .18	103.26 ± .17	137.89 ± .12	135.69 ± .03	9.39 ± .18	9.28 ± .19
AdamW	33.48 ± .68	32.22 ± .13	110.10 ± 1.32	110.72 ± 1.63	136.15 ± .21	134.68 ± .19	9.78 ± .62	9.92 ± .74
QHAdam	32.96 ± .11	30.97 ± .10	106.98 ± .25	106.18 ± .32	136.69 ± .17	134.84 ± .08	9.30 ± .23	9.24 ± .15
YellowFin	68.87 ± 5.82	50.18 ± 4.02	117.21 ± .42	109.04 ± .20	414.74 ± 5.00	351.80 ± 6.68	10.96 ± .65	10.55 ± .84
DEMON Adam	28.84 ± .18	27.11 ± .19	104.60 ± .16	107.07 ± .05	134.35 ± .24	133.98 ± .40	8.88 ± .05	8.87 ± .10

method to achieve reasonable performance with both SGDM and Adam. See Table 4.

Variational AutoEncoder(VAE-MNIST). Generative modeling is a branch of unsupervised learning that focuses on learning the underlying data distribution. VAEs [33] are generative models that pair a generator network with a recognition model that performs approximate inference and can be trained with backprop. We train VAEs on MNIST. General trends follow the ResNet settings. Interestingly, the learning rate linear schedule perform poorly with SGDM, but are improved in the Adam setting. See Table 4.

Capsule Network (CAPS-FMNIST). Capsule Networks [53] represent Neural Networks as a set of capsules that each encode a specific entity or meaning. Capsules exploit the observation that viewpoint changes significantly alter pixels but are linear with respect to the pose matrix. The activation of capsules differs from standard neural network activation functions because it depends on comparing incoming pose predictions. We train Capsule Networks on the FMNIST dataset with only Adam and its variants, which are typically used in this setting[53]. Highlighting the unpredictability

Table 5: NCSN-CIFAR10 inception score. The number of epochs was predefined before the execution of the algorithms.

	NCSN (512 epochs)
Adam	8.15 ± .20
DEMON Adam	8.07 ± .08

of the performance among learning rate schedules, the exponential learning rate decay schedule is unremarkable in other settings, but is clearly the best learning rate schedule in this setting. See Table 4.

Noise Conditional Score Network(NCSN-CIFAR10. NCSN [65] is a recent generative model that estimates gradients of the data distribution with score matching and produces samples via Langevin dynamics. We train a NCSN on CIFAR10, for which NCSN achieves a strong inception score. Although vanilla Adam achieves a slightly superior inception score (see Table 5) the results in Figure 4 are unnaturally green compared to those produced by DEMON Adam.

Table 6: Results of BERT_{BASE}-GLUE. Adam + LR Linear Schedule follows the huggingface [76] implementation, and achieves the results in well-known studies [16, 55].

	Score	CoLA	MNLI	MRPC	QNLI	QQP	RTE	SST-2	STS-B	WNLI
Adam + LR Linear Schedule	79.1	57.4	84.3	89.0	91.4	89.2	69.4	92.7	89.0	49.6
DEMON Adam	79.7	58.4	84.2	90.0	90.9	89.0	69.4	92.5	88.8	53.8

Table 7: VGG16-CIFAR100-DEMONGDM, RN20-CIFAR10-DEMONGDM generalization error, PTB-LSTM-DEMONGDM (perplexity) and VAE-MNIST-DEMONGDM generalization loss. The number of epochs was predefined before the execution.

	RN-20			VGG-16			LSTM		VAE	
	75 epochs	150 epochs	300 epochs	50 epochs	100 epochs	200 epochs	25 epochs	39 epochs	50 epochs	100 epochs
SGD ELR	9.14 ± .24	8.58 ± .08	8.16 ± .15	35.71 ± .54	30.11 ± .28	29.21 ± .32	inf	inf	inf	inf
DEMON SGDM	8.71 ± .24	7.95 ± .15	7.59 ± .12	32.26 ± .21	28.67 ± .11	27.69 ± .11	82.66 ± .105	84.84 ± .22	138.29 ± .08	136.55 ± .64

BERT(BERT_{BASE}-GLUE). BERT [16] is one of the most influential language models in the last few years. The key characteristic of BERT is the ability for a pre-trained model to be fine-tuned to achieve strong performance across a large variety of language tasks. The GLUE benchmark [68] is a collection of nine different language tasks [3, 7, 8, 14, 17, 21, 36, 49, 64, 70, 73], and is a common benchmark in NLP. We achieve the performance in well-known studies [16, 55], using the huggingface [76] default implementation of Adam with learning rate linear decay, tuning only the learning rate. We also only tune the learning rate for DEMON Adam. Results are given in Table 6. Running the same seeds, DEMON Adam yields a slight improvement over the baseline.

6 DEMON AND EFFECTIVE LEARNING RATE

We present results of Demon against the effective learning rate adjusted SGD (SGD ELR). The effective learning rate is proposed to approximate SGDM with SGD, where the learning rate is adjusted with a factor of $1/(1 - m)$ and m is the momentum coefficient. However, the results in Tables 7 demonstrate that DEMON cannot be accurately approximated with an effective learning rate adjusted SGD. For settings (PTB-LSTM-DEMONGDM and VAE-MNIST-DEMONGDM), SGD ELR causes learning to diverge. In Table 7, there exists a 0.5-3% generalization error gap for VGG16-CIFAR100 and for RN20-CIFAR10.

7 CONCLUSION

We show the effectiveness of DEMON across a large number of datasets and architectures. We demonstrate that DEMON can be effectively applied to both SGDM and Adam. Compared to other learning rate schedules and momentum schedules, DEMON achieves the largest number of Top-1 and Top-3 finishes. This includes improvements over the popular learning rate step schedule, cosine decay schedule, OneCycle, and many others. DEMON is computationally cheap, understandable, and easy to implement. We hope it is useful in practice and as a subject of future research

REFERENCES

[1] Martin Abadi, Paul Barham, Jianmin Chen, Zhifeng Chen, Andy Davis, Jeffrey Dean, Matthieu Devin, Sanjay Ghemawat, Geoffrey Irving, Michael Isard, Manjunath Kudlur, Josh Levenberg, Rajat Monga, Sherry Moore, Derek G. Murray, Benoit Steiner, Paul Tucker, Vijay Vasudevan, Pete Warden, Martin Wicke, Yuan Yu, and Xiaoqiang Zheng. 2016. TensorFlow: A system for large-scale machine

learning. In *12th USENIX Symposium on Operating Systems Design and Implementation (OSDI 16)*, 265–283. <https://www.usenix.org/system/files/conference/osdi16/osdi16-abadi.pdf>

[2] Naman Agarwal, Rohan Anil, Elad Hazan, Tomer Koren, and Cyril Zhang. 2020. Revisiting the Generalization of Adaptive Gradient Methods. (2020).

[3] Eneko Agirre, Lluís M.´arquez, and Richard Wicentowski (Eds.). 2007. *Proceedings of the Fourth International Workshop on Semantic Evaluations (SemEval-2007)*. Association for Computational Linguistics, Prague, Czech Republic.

[4] Martin Arjovsky, Soumith Chintala, and Léon Bottou. 2017. Wasserstein GAN. arXiv:1701.07875 [stat.ML]

[5] Sebastien Arnold, Pierre-Antoine Manzagol, Reza Bebanzhad, Ioannis Mitliagkas, and Nicolas Le Roux. 2019. Reducing the variance in online optimization by transporting past gradients. In *Advances in Neural Information Processing Systems*. 5392–5403.

[6] Dzmitry Bahdanau, Kyunghyun Cho, and Yoshua Bengio. 2014. Neural machine translation by jointly learning to align and translate. *arXiv preprint arXiv:1409.0473* (2014).

[7] Roy Bar Haim, Ido Dagan, Bill Dolan, Lisa Ferro, Danilo Giampiccolo, Bernardo Magnini, and Idan Szpektor. 2006. The second PASCAL recognising textual entailment challenge. (2006).

[8] Luisa Bentivogli, Ido Dagan, Hoa Trang Dang, Danilo Giampiccolo, and Bernardo Magnini. 2009. The Fifth PASCAL Recognizing Textual Entailment Challenge. (2009).

[9] Tom B. Brown, Benjamin Mann, Nick Ryder, Melanie Subbiah, Jared Kaplan, Prafulla Dhariwal, Arvind Neelakantan, Pranav Shyam, Girish Sastry, Amanda Askell, Sandhini Agarwal, Ariel Herbert-Voss, Gretchen Krueger, Tom Henighan, Rewon Child, Aditya Ramesh, Daniel M. Ziegler, Jeffrey Wu, Clemens Winter, Christopher Hesse, Mark Chen, Eric Sigler, Mateusz Litwin, Scott Gray, Benjamin Chess, Jack Clark, Christopher Berner, Sam McCandlish, Alec Radford, Ilya Sutskever, and Dario Amodei. 2020. Language Models are Few-Shot Learners. arXiv:2005.14165 [cs.CL]

[10] Jinghui Chen and Quanquan Gu. 2018. Closing the generalization gap of adaptive gradient methods in training deep neural networks. *arXiv preprint arXiv:1806.06763* (2018).

[11] Jianmin Chen, Xinghao Pan, Rajat Monga, Samy Bengio, and Rafal Jozefowicz. 2016. Revisiting distributed synchronous SGD. *arXiv preprint arXiv:1604.00981* (2016).

[12] Dami Choi, Christopher J. Shallue, Zachary Nado, Jaehoon Lee, Chris J. Maddison, and G. Dahl. 2019. On Empirical Comparisons of Optimizers for Deep Learning. *ArXiv abs/1910.05446* (2019).

[13] Ashok Cutkosky and Francesco Orabona. 2019. Momentum-Based Variance Reduction in Non-Convex SGD. *arXiv preprint arXiv:1905.10018* (2019).

[14] Ido Dagan, Oren Glickman, and Bernardo Magnini. 2006. The PASCAL recognising textual entailment challenge. In *Machine learning challenges. evaluating predictive uncertainty, visual object classification, and recognising textual entailment*. Springer, 177–190.

[15] Aaron Defazio and Robert M. Gower. 2020. Factorial Powers for Stochastic Optimization. arXiv:2006.01244 [cs.LG]

[16] Jacob Devlin, Ming-Wei Chang, Kenton Lee, and Kristina Toutanova. 2019. BERT: Pre-training of Deep Bidirectional Transformers for Language Understanding. arXiv:1810.04805 [cs.CL]

[17] William B Dolan and Chris Brockett. 2005. Automatically constructing a corpus of sentential paraphrases. In *Proceedings of the International Workshop on Paraphrasing*.

- [18] John Duchi, Elad Hazan, and Yoram Singer. 2011. Adaptive subgradient methods for online learning and stochastic optimization. *Journal of Machine Learning Research* 12, Jul (2011), 2121–2159.
- [19] Jonas Gehring, Michael Auli, David Grangier, Denis Yarats, and Yann N Dauphin. 2017. Convolutional sequence to sequence learning. In *Proceedings of the 34th International Conference on Machine Learning-Volume 70*. JMLR. org, 1243–1252.
- [20] Euhanna Ghadimi, Hamid Reza Feyzmahdavian, and Mikael Johansson. 2014. Global Convergence of the HeavyBall Method for Convex Optimization. *arXiv preprint arXiv:1412.7457* (2014).
- [21] Danilo Giampiccolo, Bernardo Magnini, Ido Dagan, and Bill Dolan. 2007. The third PASCAL recognizing textual entailment challenge. In *Proceedings of the ACL-PASCAL workshop on textual entailment and paraphrasing*. Association for Computational Linguistics, 1–9.
- [22] Gauthier Gidel, Reyhane Askari Hemmat, Mohammad Pezeshki, Remi Lepril, Gabriel Huang, Simon Lacoste-Julien, and Ioannis Mitliagkas. 2018. Negative momentum for improved game dynamics. *arXiv preprint arXiv:1807.04740* (2018).
- [23] Kaiming He, Xiangyu Zhang, Shaoqing Ren, and Jian Sun. 2016. Deep residual learning for image recognition. In *Proceedings of the IEEE conference on computer vision and pattern recognition*. 770–778.
- [24] Byeongho Heo, Sanghyuk Chun, Seong Joon Oh, Dongyoon Han, Sangdoon Yun, Gyuwan Kim, Youngjung Uh, and Jung-Woo Ha. 2020. AdamP: Slowing Down the Slowdown for Momentum Optimizers on Scale-invariant Weights. *arXiv:2006.08217* [cs.LG]
- [25] Geoffrey Hinton, Nitish Srivastava, and Kevin Swersky. 2012. Neural networks for machine learning lecture 6a overview of mini-batch gradient descent. *Cited on 14* (2012), 8.
- [26] Sepp Hochreiter and Jürgen Schmidhuber. 1997. Long short-term memory. *Neural computation* 9, 8 (1997), 1735–1780.
- [27] Andrew G Howard, Menglong Zhu, Bo Chen, Dmitry Kalenichenko, Weijun Wang, Tobias Weyand, Marco Andreetto, and Hartwig Adam. 2017. Mobilenets: Efficient convolutional neural networks for mobile vision applications. *arXiv preprint arXiv:1704.04861* (2017).
- [28] Jie Hu, Li Shen, Samuel Albanie, Gang Sun, and Enhua Wu. 2017. Squeeze-and-excitation networks. *arxiv preprint arXiv:1709.01507* (2017).
- [29] Gao Huang, Zhuang Liu, Laurens Van Der Maaten, and Kilian Q Weinberger. 2017. Densely connected convolutional networks. In *Proceedings of the IEEE conference on computer vision and pattern recognition*. 4700–4708.
- [30] Prateek Jain, Sham M. Kakade, Rahul Kidambi, Praneeth Netrapalli, and Aaron Sidford. 2017. Accelerating Stochastic Gradient Descent For Least Squares Regression. *arXiv preprint arXiv:1704.08227* (2017).
- [31] Rahul Kidambi, Praneeth Netrapalli, Prateek Jain, and Sham Kakade. 2018. On the insufficiency of existing momentum schemes for stochastic optimization. In *2018 Information Theory and Applications Workshop (ITA)*. IEEE, 1–9.
- [32] Diederik P Kingma and Jimmy Ba. 2014. Adam: A method for stochastic optimization. *arXiv preprint arXiv:1412.6980* (2014).
- [33] Diederik P Kingma and Max Welling. 2015. Auto-encoding variational Bayes. *arXiv preprint arXiv:1312.6114* (2015).
- [34] Alex Krizhevsky, Ilya Sutskever, and Geoffrey E Hinton. 2012. Imagenet classification with deep convolutional neural networks. In *Advances in neural information processing systems*. 1097–1105.
- [35] Laurent Lessard, Benjamin Recht, and Andrew Packard. 2016. Analysis and design of optimization algorithms via integral quadratic constraints. *SIAM Journal on Optimization* 26, 1 (2016), 57–95.
- [36] Hector J Levesque, Ernest Davis, and Leora Morgenstern. 2011. The Winograd schema challenge. In *AAAI Spring Symposium: Logical Formalizations of Commonsense Reasoning*, Vol. 46. 47.
- [37] Tsung-Yi Lin, Piotr Dollar, Ross Girshick, Kaiming He, Bharath Hariharan, and Serge Belongie. 2017. Feature pyramid networks for object detection. *CVPR* (2017).
- [38] Ilya Loshchilov and Frank Hutter. 2017. Fixing weight decay regularization in adam. *arXiv preprint arXiv:1711.05101* (2017).
- [39] Ilya Loshchilov and Frank Hutter. 2017. SGDR: Stochastic Gradient Descent with Warm Restarts. *arXiv:1608.03983* [cs.LG]
- [40] James Lucas, Shengyang Sun, Richard Zemel, and Roger Grosse. 2018. Aggregated momentum: Stability through passive damping. *arXiv preprint arXiv:1804.00325* (2018).
- [41] Jerry Ma and Denis Yarats. 2018. Quasi-hyperbolic momentum and Adam for deep learning. *arXiv preprint arXiv:1810.06801* (2018).
- [42] Tomas Mikolov, Ilya Sutskever, Kai Chen, Greg S Corrado, and Jeff Dean. 2013. Distributed representations of words and phrases and their compositionality. In *Advances in neural information processing systems*. 3111–3119.
- [43] Mehdi Mirza and Simon Osindero. 2014. Conditional generative adversarial nets. *arXiv preprint arXiv:1411.1784* (2014).
- [44] Ioannis Mitliagkas, Ce Zhang, Stefan Hadjis, and Christopher Ré. 2016. Asynchrony begets momentum, with an application to deep learning. In *2016 54th Annual Allerton Conference on Communication, Control, and Computing (Allerton)*. IEEE, 997–1004.
- [45] Yurii Nesterov. 1983. A method for solving the convex programming problem with convergence rate of $(1/k)^2$. *Soviet Mathematics Doklady* 27, 2 (1983), 372–376.
- [46] Brendan O’donoghue and Emmanuel Candes. 2015. Adaptive restart for accelerated gradient schemes. *Foundations of computational mathematics* 15, 3 (2015), 715–732.
- [47] Adam Paszke, Sam Gross, Soumith Chintala, Gregory Chanan, Edward Yang, Zachary DeVito, Zeming Lin, Alban Desmaison, Luca Antiga, and Adam Lerer. 2017. Automatic differentiation in PyTorch. (2017).
- [48] Alec Radford, Luke Metz, and Soumith Chintala. 2015. Unsupervised representation learning with deep convolutional generative adversarial networks. *arXiv preprint arXiv:1511.06434* (2015).
- [49] Pranav Rajpurkar, Jian Zhang, Konstantin Lopyrev, and Percy Liang. 2016. SQuAD: 100,000+ Questions for Machine Comprehension of Text. In *Proceedings of EMNLP* (Austin, Texas). Association for Computational Linguistics, 2383–2392.
- [50] Sashank J Reddi, Satyen Kale, and Sanjay Kumar. 2019. On the convergence of Adam and beyond. *arXiv preprint arXiv:1904.09237* (2019).
- [51] Shaoqing Ren, Kaiming He, Ross Girshick, and Jian Sun. 2015. Faster R-CNN: Towards real-time object detection with region proposal networks. In *Advances in neural information processing systems*. 91–99.
- [52] Sebastian Ruder. 2016. An overview of gradient descent optimization algorithms. *arXiv preprint arXiv:1609.04747* (2016).
- [53] Sara Sabour, Nicholas Fross, and Geoffrey Hinton. 2017. Dynamic routing between capsules. In *Advances in neural information processing systems*.
- [54] Haşim Sak, Andrew Senior, and Françoise Beaufays. 2014. Long short-term memory recurrent neural network architectures for large scale acoustic modeling. In *Fifteenth annual conference of the international speech communication association*.
- [55] Victor Sanh, Lysandre Debut, Julien Chaumond, and Thomas Wolf. 2020. DistilBERT, a distilled version of BERT: smaller, faster, cheaper and lighter. *arXiv:1910.01108* [cs.CL]
- [56] Tom Sercu, Christian Puhresch, Brian Kingsbury, and Yann LeCun. 2016. Very deep multilingual convolutional neural networks for LVCSR. In *2016 IEEE International Conference on Acoustics, Speech and Signal Processing (ICASSP)*. IEEE, 4955–4959.
- [57] Vatsal Shah, Anastasios Kyrillidis, and Sujay Sanghavi. 2018. Minimum norm solutions do not always generalize well for over-parameterized problems. *arXiv preprint arXiv:1811.07055* (2018).
- [58] Vaishaal Shankar, Rebecca Roelofs, Horia Mania, Alex Fang, Benjamin Recht, and Ludwig Schmidt. 2020. Evaluating Machine Accuracy on ImageNet. In *Proceedings of the 37th International Conference on Machine Learning (Proceedings of Machine Learning Research, Vol. 119)*, Hal Daumé III and Aarti Singh (Eds.). PMLR, 8634–8644. <http://proceedings.mlr.press/v119/shankar20c.html>
- [59] Or Sharir, Barak Peleg, and Yoav Shoham. 2020. The Cost of Training NLP Models: A Concise Overview. *arXiv preprint arXiv:2004.08900* (2020).
- [60] Karen Simonyan and Andrew Zisserman. 2014. Very deep convolutional networks for large-scale image recognition. *arXiv preprint arXiv:1409.1556* (2014).
- [61] Prabhuv Sivasubramanian, Florian Mai, Thijs Vogels, Martin Jaggi, and François Fleuret. 2019. On the Tunability of Optimizers in Deep Learning. (10 2019).
- [62] Leslie Smith. 2018. A disciplined approach to neural network hyper-parameters: Part 1 – learning rate, batch size, momentum, and weight decay. *arXiv preprint arXiv:1803.09820* (2018).
- [63] Samuel Smith, Pieter-Jan Kindermans, Chris Ying, and Quoc Le. 2017. Don’t Decay the Learning Rate, Increase the Batch Size. *arXiv preprint arXiv:1711.00489* (2017).
- [64] Richard Socher, Alex Perelygin, Jean Wu, Jason Chuang, Christopher D Manning, Andrew Ng, and Christopher Potts. 2013. Recursive deep models for semantic compositionality over a sentiment treebank. In *Proceedings of EMNLP*. 1631–1642.
- [65] Yang Song and Stefano Ermon. 2019. Generative Modeling by Estimating Gradients of the Data Distribution. *arXiv preprint arXiv:1907.05600* (2019).
- [66] Vishwak Srinivasan, Adepu Ravi Sankar, and Vineeth N Balasubramanian. 2018. ADINE: an adaptive momentum method for stochastic gradient descent. In *Proceedings of the ACM India Joint International Conference on Data Science and Management of Data*. ACM, 249–256.
- [67] Ilya Sutskever, James Martens, George Dahl, and Geoffrey Hinton. 2013. On the importance of initialization and momentum in deep learning. In *International conference on machine learning*. 1139–1147.
- [68] Alex Wang, Amanpreet Singh, Julian Michael, Felix Hill, Omer Levy, and Samuel R. Bowman. 2019. GLUE: A Multi-Task Benchmark and Analysis Platform for Natural Language Understanding. In the Proceedings of ICLR.
- [69] Fei Wang, Mengqing Jiang, Chen Qian, Shuo Yang, Cheng Li, Honggang Zhang, Xiaogang Wang, and Xiaoou Tang. 2017. Residual attention network for image classification. *CVPR* (2017).
- [70] Alex Warstadt, Amanpreet Singh, and Samuel R. Bowman. 2018. Neural Network Acceptability Judgments. *arXiv preprint 1805.12471* (2018).
- [71] Andre Wibisono and Ashia C Wilson. 2015. On accelerated methods in optimization. *arXiv preprint arXiv:1509.03616* (2015).
- [72] Andre Wibisono, Ashia C Wilson, and Michael I Jordan. 2016. A variational perspective on accelerated methods in optimization. *proceedings of the National Academy of Sciences* 113, 47 (2016), E7351–E7358.

- [73] Adina Williams, Nikita Nangia, and Samuel R. Bowman. 2018. A Broad-Coverage Challenge Corpus for Sentence Understanding through Inference. In *Proceedings of NAACL-HLT*.
- [74] Ashia C Wilson, Benjamin Recht, and Michael I Jordan. 2016. A Lyapunov analysis of momentum methods in optimization. *arXiv preprint arXiv:1611.02635* (2016).
- [75] Ashia C Wilson, Rebecca Roelofs, Mitchell Stern, Nati Srebro, and Benjamin Recht. 2017. The marginal value of adaptive gradient methods in machine learning. In *Advances in Neural Information Processing Systems*. 4148–4158.
- [76] Thomas Wolf, Lysandre Debut, Victor Sanh, Julien Chaumond, Clement Delangue, Anthony Moi, Pierric Cistac, Tim Rault, Rémi Louf, Morgan Funtowicz, Joe Davison, Sam Shleifer, Patrick von Platen, Clara Ma, Yacine Jernite, Julien Plu, Canwen Xu, Teven Le Scao, Sylvain Gugger, Mariama Drame, Quentin Lhoest, and Alexander M. Rush. 2020. HuggingFace’s Transformers: State-of-the-art Natural Language Processing. *arXiv:1910.03771* [cs.CL]
- [77] Saining Xie, Ross Girshick, Piotr Dollár, Zhuowen Tu, and Kaiming He. 2017. Aggregated residual transformations for deep neural networks. In *Proceedings of the IEEE conference on computer vision and pattern recognition*. 1492–1500.
- [78] Kun Yuan, Bicheng Ying, and Ali Sayed. 2016. On the influence of momentum acceleration on online learning. *Journal of Machine Learning Research* 17, 192 (2016), 1–66.
- [79] Sergey Zagoruyko and Nikos Komodakis. 2016. Wide residual networks. *arXiv preprint arXiv:1605.07146* (2016).
- [80] Matthew D Zeiler. 2012. ADADELTA: an adaptive learning rate method. *arXiv preprint arXiv:1212.5701* (2012).
- [81] Jian Zhang and Ioannis Mitliagkas. 2017. Yellowfin and the art of momentum tuning. *arXiv preprint arXiv:1706.03471* (2017).
- [82] Fangyu Zou, Li Shen, Zequn Jie, Weizhong Zhang, and Wei Liu. 2018. A sufficient condition for convergences of Adam and RMSProp. *arxiv preprint arXiv:1811.09358* (2018).

A EXPERIMENTS

We describe the nine test problems in this paper.

- **CIFAR10 - ResNet20.** CIFAR10 contains 60,000 32x32x3 images with a 50,000 training set, 10,000 test set split. There are 10 classes. ResNet20 [23] is a 20 layers deep CNN with skip connections for image classification. Trained with a batch size of 128.
- **TINY IMAGENET - ResNet56.** Tiny ImageNet contains 110,000 64x64x3 images with a 100,000 training set, 10,000 test set split. There are 200 classes. ResNet56 [23] is a 56 layer deep CNN with skip connections for image classification. Trained with a batch size of 128.
- **CIFAR100 - VGG16.** CIFAR100 is a fine-grained version of CIFAR-10 and contains 60,000 32x32x3 images with a 50,000 training set, 10,000 test set split. There are 100 classes. VGG16 [60] is a 16 layers deep CNN with extensive use of 3x3 convolutional filters. Trained with a batch size of 128.
- **STL10 - Wide ResNet 16-8.** STL10 contains 1300 96x96x3 images with a 500 training set, 800 test set split. There are 10 classes. Wide ResNet 16-8 [79] is a 16 layers deep ResNet which is 8 times wider. Trained with a batch size of 64.
- **PTB - LSTM.** PTB is an English text corpus containing 929,000 training words, 73,000 validation words, and 82,000 test words. There are 10,000 words in the vocabulary. The model is stacked LSTMs [26] with 2 layers, 650 units per layer, and dropout of 0.5. Trained with a batch size of 20. We use the official TensorFlow v1 implementation for PTB - LSTM.
- **FMNIST - CAPS.** FMNIST contains 60,000 32x32x1 grayscale images with a 50,000 training set, 10,000 test set split. There are 10 classes of 10 clothing items. Capsule Networks [53] represent Neural Networks as a set of capsules, where each capsule encodes a specific entity or meaning. The activations of capsules depend on comparing incoming pose predictions, as opposed to standard neural networks. The Capsule Network uses 3 iterations in the routing algorithm. Trained with a batch size of 128.
- **MNIST - VAE.** MNIST contains 60,000 32x32x1 grayscale images with a 50,000 training set, 10,000 test set split. There are 10 classes of 10 digits. VAE [33] with three dense encoding layers and three dense decoding layers with a latent space of size 2. Trained with a batch size of 100.
- **CIFAR10 - NCSN.** CIFAR10 contains 60,000 32x32x3 images with a 50,000 training set, 10,000 test set split. There are 10 classes. NCSN [65] is a recent state-of-the-art generative model which achieves the best reported inception score. We compute inception scores based on a total of 50000 samples. Since DEMON depends on a predefined number of epochs, we evaluate inception score at the end of training; otherwise, we follow the exact implementation in and defer details to the original paper.
- **GLUE - BERT.** The GLUE benchmark [68] consists of 9 different language tasks [3, 7, 8, 14, 17, 21, 36, 49, 64, 70, 73], grouped together to form a benchmark. BERT [16] is a relatively recently proposed language model which has become the standard for many tasks in NLP. In particular, BERT can be fine-tuned to an array of tasks, and here we evaluate the fine-tuning procedure of BERT to the GLUE benchmark.